FULL PAPER

Photo- and pH-Triggered Release of Anticancer Drugs from Mesoporous Silica-Coated Pd@Ag Nanoparticles

*Weijun Fang, Jing Yang, Jiawei Gong, and Nanfeng Zheng**

A smart drug delivery system integrating both photothermal therapy and chemotherapy for killing cancer cells is reported. The delivery system is based on a mesoporous silica-coated Pd@Ag nanoplates composite. The Pd@Ag nanoplate core can effectively absorb and convert near infrared (NIR) light into heat. The mesoporous silica shell is provided as the host for loading anticancer drug, doxorubicin (DOX). The mesoporous shell consists of large pores, ~10 nm in diameter, and allows the DOX loading as high as 49% in weight. DOX loaded core–shell nanoparticles exhibit a higher efficiency in killing cancer cells than free DOX. More importantly, DOX molecules are loaded in the mesopores shell through coordination bonds that are responsive to pH and heat. The release of DOX from the core-shell delivery vehicles into cancer cells can be therefore triggered by the pH drop caused by endocytosis and also NIR irradiation. A synergistic effect of combining chemotherapy and photothermal therapy is observed in our core-shell drug delivery system. The cell-killing efficacy by DOX-loaded core–shell particles under NIR irradiation is higher than the sum of chemotherapy by DOX-loaded particles and photothermal therapy by core–shell particles without DOX.

1. Introduction

Drug delivery with controllable release using nanoscale carriers is a very important research area in biomedical sciences.[1] Polymer-based carriers have been used as smart drug delivery systems for decades, and some polymer carriers have been approved for human clinical use by the U.S. Food and Drug Administration.[2] Due to their possible enhanced stability in biological systems, inorganic-based vectors used for biomedical applications have attracted increasing research attention in the past years.

Among inorganic-based materials, mesoporous silica nanoparticles (MSNs) are advantagenous in the area of drug controllable release in that they display excellent stability, non-cytotoxicity, tunable porosity and facile modification.[3] To apply MSNs as effective carriers for drug controllable release, various strategies have been developed by introducing labile chemical bonds or interactions in the system. These bonds and interactions can respond to external agents and conditions, such as salt concentration,[4] pH,[5] temperature,[6] enzyme/DNA,[7] reducing biomolecules,[8] light[9] and so on. Among them, light-responsive controlled release is a very important method because of the non-invasive nature and high spatial resolution of light. For instance, the release of guest molecules in MCM-41 nanoparticles could be triggered by UV irradiation using coumarin dimers as the photo-cleavable molecular gates.[10] A similar control strategy was achieved by modifying the pores of MSNs with azobenzene derivatives which could undergo *cis–trans* isomerization under laser irradiation at 412 nm.[11] The other approach is to use polymers or gold nanoparticles to block the pores of MSNs.[12] Under ultraviolet–visible (UV–vis) light irradiation, the pores could be opened to release the drug molecules loaded inside the mesopores. Owing to its low penetrability and harm to tissue, however, ultraviolet/visible light for drug controllable release has received limited use in in vivo applications. In comparison with UV–vis light, near-infrared (NIR) light can deeply penetrate tissues.[13] To control the drug release using NIR, several groups have modified MSNs by attaching drug molecules or nanoparticles through NIR light sensitive covalent bonding.[14]

Based on mesoporous silica-coated Pd@Ag nanoplates, we now report a smart drug delivery system integrating both photothermal therapy and chemotherapy for killing cancer cells. While the Pd@Ag nanoplate core can effectively absorb and convert NIR light into heat, the mesoporous silica shell is provided as the host for loading anticancer drug, doxorubicin (DOX). Three important features are associated with our delivery system: 1) Unlike many reported Au/Ag nanostructures that could melt themselves into spheres upon NIR irradiation, the Pd@Ag nanoplates that are used as the core in our system exhibit excellent photothermal stability.[15,16] 2) The mesoporous shell consists of large pores, ~10 nm in diameter. The enlarged pore offers significantly improved drug loading capacity. The DOX loading in our delivery vehicles is as high as 49% in weight. 3) DOX molecules are loaded in the mesoporous shell through coordination bonds that are responsive to pH and heat. In physiological pH (~7.4), DOX molecules are barely released from the vehicles. But the DOX release can be released easily once local pH decreases, which always happens

W. J. Fang, Dr. J. Yang, J. W. Gong, Prof. N. F. Zheng
State Key Laboratory for Physical Chemistry of Solid Surfaces
and Department of Chemistry
College of Chemistry and Chemical Engineering
Xiamen University
Xiamen 361005, P. R. China
E-mail: nfzheng@xmu.edu.cn

DOI: 10.1002/adfm.201101960

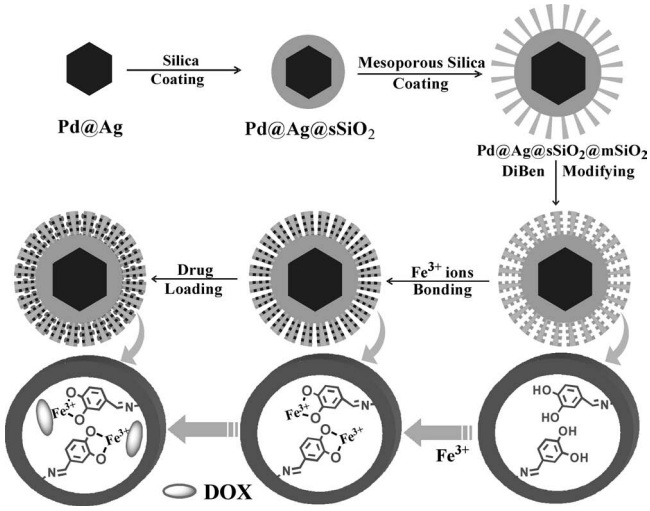

Scheme 1. Synthetic Process of Pd@Ag@sSiO$_2$@mSiO$_2$-DihBen/DOX Nanocomposites.

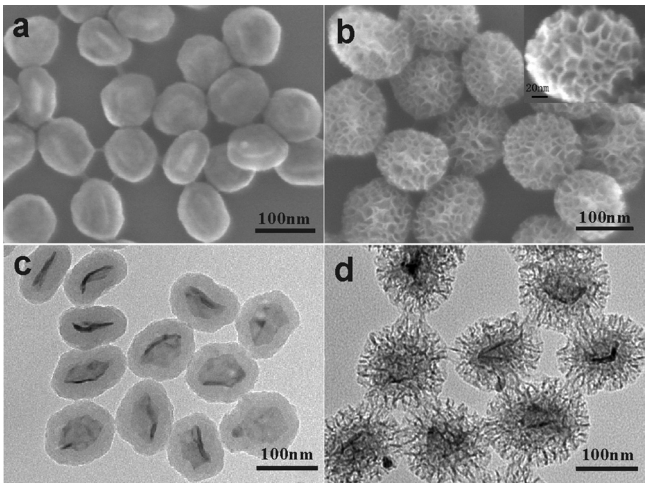

Figure 1. SEM (a,b) and TEM (c,d) images of Pd@Ag@sSiO$_2$ and Pd@Ag@sSiO$_2$ @mSiO$_2$ nanoparticles.

when the particles are endocytosed by cancer cells. With the incorporation of the Pd@Ag photothermal core in the delivery system, the release of DOX can also be triggered by NIR irradiation. Our in vitro experiments reveal a synergistic effect that the cell-killing efficacy by DOX-loaded core-shell particles under NIR irradiation is even higher than the sum of chemotherapy by DOX-loaded particles and photothermal therapy by core-shell particles without DOX.

2. Results and Discussion

Scheme 1 shows the procedure for the synthesis of mesoporous silica-coated Pd@Ag nanoparticles. The Pd@Ag nanoplates with a mean diameter of 41 nm and a Ag/Pd ratio of 2.1 were first prepared according to our recently reported method.[16] Compared with Ag/Au nanoplates, these Pd@Ag nanoplates exhibit significantly enhanced photothermal stability under NIR irradiation. Before coating the Pd@Ag nanoplates with mesoporous silica, a layer of dense silica was grown on the nanoplates using a modified Stöber method (see the Experimental Section for details). As shown in **Figure 1** (and Figure S1 in the Supporting Information), the obtained Pd@Ag@sSiO$_2$ particles were oblate spheroids with an average diameter of 110 nm and a thickness of 60 nm. A mesoporous silica was then deposited on Pd@Ag@sSiO$_2$ particles using a modified method reported by Tatsumi et al.[17] In our synthesis, the amount of L-Arginine (Arg) was reduced to decrease the rate of reaction and trimethylbenzene (TMB) was introduced as a swelling agent for the CTAC micelles to enlarge the pores. The growth of mesoporous silica around the Pd@Ag@sSiO$_2$ core was also evidenced by both SEM and TEM analysis. The formation of the mesoporous silica shell should consist two main steps:[18] 1) The CTAC micelles were firstly adsorbed on the surface of Pd@Ag@sSiO$_2$ particles by electrostatic interaction. 2) Silica was then co-assembled with CTCA to form the mesostructure under weakly basic conditions. The as-prepared Pd@Ag@sSiO$_2$@mSiO$_2$ particles had an average diameter of ~150 nm. The pores in the mesoporous shells were ~10 nm, much larger than the typical pores in MCM-41 made in the absence of swelling agent. The enlarged pores were also confirmed by our N_2 adsorption–desorption experiments (**Figure 2**). The isotherm of Pd@Ag@sSiO$_2$@mSiO$_2$ after CTAC extraction shows a typical type IV feature. The BET (Brunauer–Emmett–Teller) surface area and pore volume of the core–shell nanoparticles were measured to be 489 m^2 g^{-1} and 0.972 m^3 g^{-1}, respectively. The average pore diameter was calculated to be 10 nm from the desorption branch of the isotherm by using the Barrett–Joyner–Halenda (BJH) model.

After the creation of the mesoporous shell, CTAC molecules in the pore were removed by an ion-exchange method. As shown in the infrared spectra of CTAC, Pd@Ag@sSiO$_2$@mSiO$_2$/CTAC and Pd@Ag@sSiO$_2$@mSiO$_2$ (**Figure 3**), the

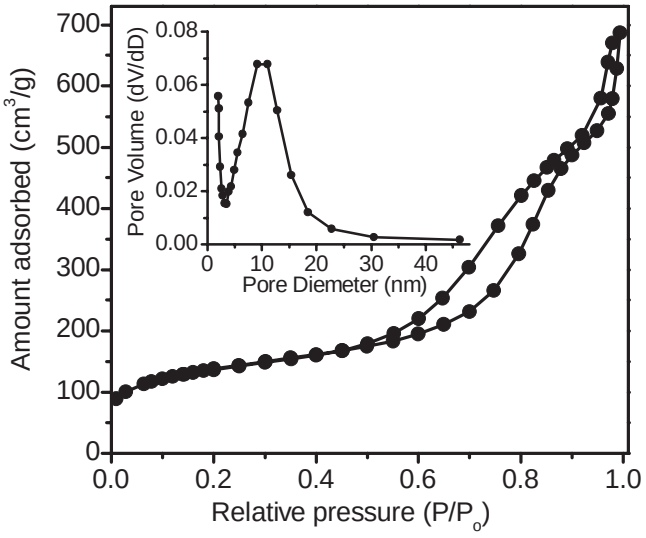

Figure 2. N_2 adsorption/desorption isotherm and the pore size distribution (inset) of Pd@Ag@sSiO$_2$@mSiO$_2$ nanoparticles.

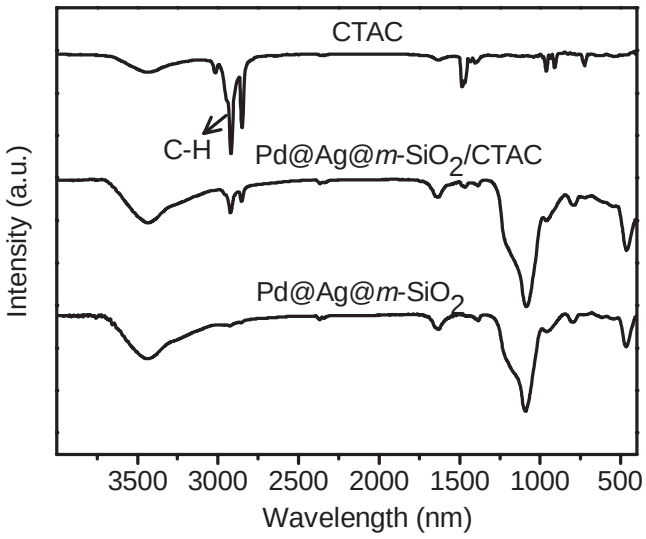

Figure 3. IR spectra of CTAC (top curve), Pd@Ag@sSiO$_2$@mSiO$_2$/CTAC (middle curve) and Pd@Ag@sSiO$_2$@mSiO$_2$ (bottom curve).

strong absorption bands around 2920 cm^{-1} and 2849 cm^{-1} were assigned the stretching of the C–H bonds of the CTAC molecules. After ion exchange with NH_4NO_3, the strong absorption bands disappeared, suggesting that the CTAC molecules had been removed successfully. The particles were then modified with amino groups by reacting with 3-aminopropyltriethoxysilane (APTES) (see the Experimental Section for details). These amino-bearing particles were reacted with 3,4-dihydroxybenzaldehyde (DihBen) to yield Pd@Ag@sSiO$_2$@mSiO$_2$-DihBen particles. As shown in **Figure 4**, the apparent absorption bands around at 1380 cm^{-1}, 1465 cm^{-1} and 2953 cm^{-1}, which were assigned to aromatic C-C (arC–C) and C–H bonds respectively, suggested that the DihBen motifs were successfully anchored

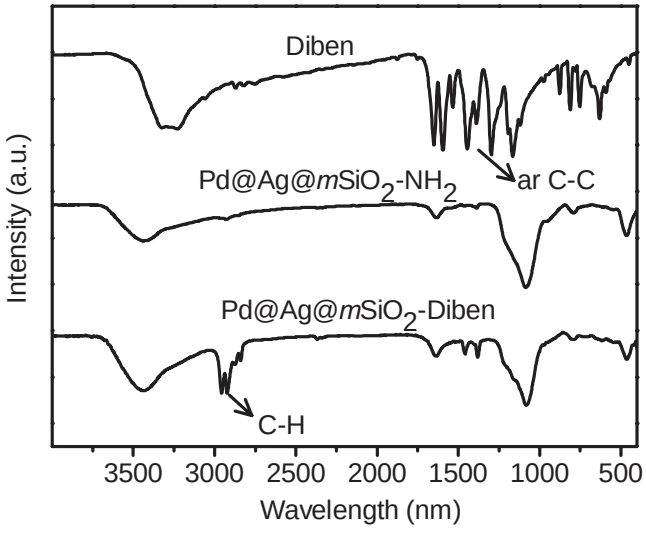

Figure 4. IR spectra of 3,4-dihydroxybenzaldehyde (top curve), Pd@Ag@sSiO$_2$@mSiO$_2$ (middle curve) and Pd@Ag@sSiO$_2$@mSiO$_2$-DihBen (bottom curve).

onto the Pd@Ag@sSiO$_2$@mSiO$_2$ particles. Subsequently, Fe^{3+} ions were bound to the dihydroxybenzene motifs. Finally, DOX molecules were loaded onto the pore walls through –NH_2–Fe^{3+} coordination.[19] The loading of DOX on the Fe^{3+}-immobilized particles was evaluated by monitoring the fluorescence of the DOX solutions treated with the core–shell nanoparticles. After loaded on the particles, the fluorescence of DOX was quenched, which was also previously observed when they were loaded on other nanocarriers.[20] Based on the change of fluorescence intensity (**Figure 5**a), the loading of DOX on Pd@Ag@sSiO$_2$@mSiO$_2$-DihBen-Fe^{3+} was calculated as high as 49 wt% related to the weight of core–shell mesoporous carriers.[20b] Such a high DOX loading has not been reported for MSNs. In comparison, the adsorption amount of DOX for pure Pd@Ag nanoplates and Pd@Ag@sSiO$_2$ nanoparticles was only 1.9 wt% and 3.9 wt%, respectively. It is believed that the enhanced DOX loading capacity of Pd@Ag@sSiO$_2$@mSiO$_2$-DihBen-Fe^{3+} is due to the enlarged mesopores in favor of DOX, which are rather large drug molecules (1.53 nm × 1.19 nm).

DOX molecules are bound to the Pd@Ag@sSiO$_2$@mSiO$_2$-DihBen-Fe^{3+} particles through -NH_2-Fe^{3+} coordination bonds. Considering that –NH_2–Fe^{3+} bonds are fairly stable under neutral condition but prone to be attacked by acids, one would expect a pH-controllable release of DOX loaded on Pd@Ag@sSiO$_2$@mSiO$_2$-DihBen-Fe^{3+}. Indeed, as clearly shown in Figure 5b, both the amount and the rate of DOX release in PBS buffers highly depend on the pH values. Within 8 h, only 7.2% of the DOX adsorbed on the particles was released. Lowering the pH to 6.0, 5.0, and 4.0 increased the DOX release to 17%, 26%, and 36%, respectively.

As described above, one key feature of our core-shell delivery system lies in the Pd@Ag nanoplate core that can effectively absorb and convert NIR light into heat. As shown in Figure 5c, even after silica coating, the strong NIR absorption feature of Pd@Ag nanoplates was nicely kept although the absorption peak became slightly broader. Under laser irradiation of 1 W at 808 nm, the temperature of 1 mL solution containing 200 ppm (weight of all components) Pd@Ag@sSiO$_2$@mSiO$_2$-DihBen-Fe^{3+} nanoparticles was raised from 27.1 to 51.7 °C (Figure 5d). The bond strength of coordination typically decreases with temperature. Therefore, a temperature increase resulted from the photothermal effect by the Pd@Ag core would help to release more DOX molecules from Pd@Ag@sSiO$_2$@mSiO$_2$-DihBen-Fe^{3+} nanoparticles. Indeed, a significant promotion effect of NIR irradiation on the DOX release was observed experimentally (**Figure 6**). At pH 4, irradiation with a 1 W, 808 nm NIR laser increased the DOX release up to 63.2% within 1 h. In comparison, only 33.5% DOX was released without the irradiation. At pH 7.4, an increase of 1 h DOX release from 3.8 to 9.6% was also achieved by NIR irradiation. These results verify that the core–shell mesoporous nanoparticles have successfully achieved the drug controllable release by pH and NIR light.

The success in controlling the DOX release by both pH and NIR laser motivated us to examine whether the delivery system would work in living cells. We first examined the biocompatibility of the Pd@Ag@sSiO$_2$@mSiO$_2$-DihBen particles by incubating Hep-G2 cells with the nanoparticles at different concentrations for 24 h. As revealed by the 3-(4,5-dimethylthiazol-2-yl)-2,5-diphenyltetrazolium bromide (MTT) assay, the

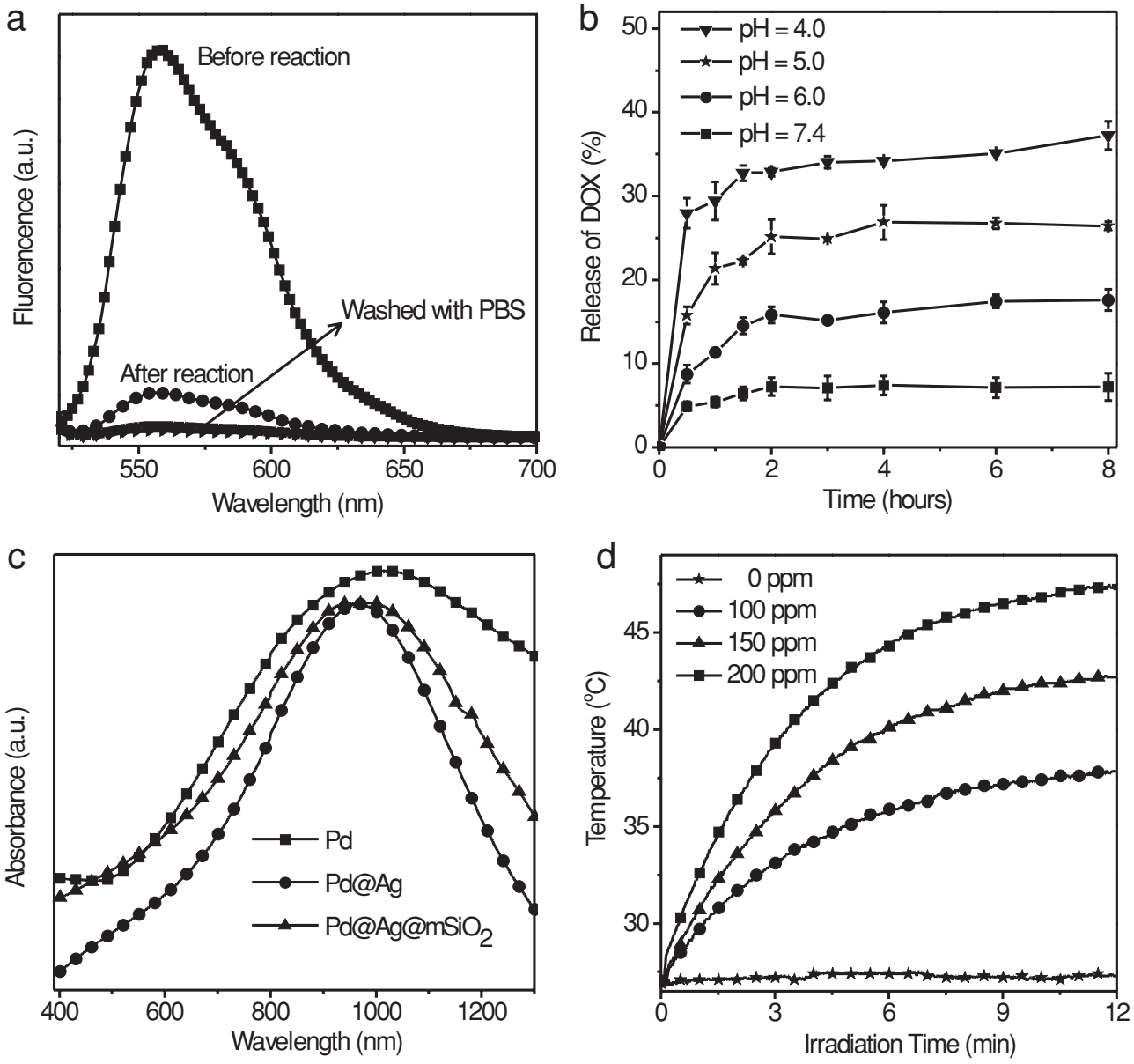

Figure 5. a) Fluorescence spectra showing the change of emission intensity of the solutions of DOX before and after treated with Pd@Ag@sSiO$_2$@mSiO$_2$-DihBen-Fe^{3+} nanoparticles. b) Release kinetics of DOX from Pd@Ag@sSiO$_2$@mSiO$_2$ in PBS buffer at different pH values. c) UV–vis spectra of Pd, Pd@Ag and Pd@Ag@sSiO$_2$@mSiO$_2$ nanoparticles in water solution. d) Temperature versus time plots of 1 mL solutions containing Pd@Ag@sSiO$_2$@mSiO$_2$-DihBen-Fe^{3+} nanoparticles in various concentrations under laser irradiation of 1 W at 808 nm.

viability of the cells was only reduced by ~20% after 24 h NIR exposure to a Pd@Ag@sSiO$_2$@mSiO$_2$-DihBen-Fe^{3+} dispersion containing 200 ppm particles (**Figure 7**a). Based on these cytotoxicity data, we have limited the amount of Pd@Ag @sSiO$_2$@mSiO$_2$-DihBen in our cell studies to less than 200 ppm.

In contrast to DOX loaded on Pd@Ag@sSiO$_2$@mSiO$_2$-DihBen-Fe^{3+}, free DOX molecules are highly fluorescent, allowing us to use fluorescence microscopy to monitor the drug release inside living cells. Before fluorescence microscopy was performed, Hep-G2 cells were first incubated with DOX loaded nanoparticles (20 ppm DOX) for 4 h and then washed with PBS. As clearly revealed by fluorescence microscopy images (Figure S2 in the Supporting Information), intense fluorescence signals were observed inside the cells. Since the fluorescence of DOX was significantly quenched when loaded on the particles, the appearance of fluorescence signals inside the cells indicated the actual release of DOX from the Pd@Ag@sSiO$_2$@mSiO$_2$-DihBen-Fe^{3+}. It should be noted that the fluorescence signals inside the cells incubated with the same concentration of free DOX for 4 h were much weaker (Figure S2). This result indicates that the Pd@Ag@sSiO$_2$@mSiO$_2$-DihBen-Fe^{3+} particles help the DOX delivery into Hep-G2 cells.

With no doubt, the improved DOX delivery efficacy by Pd@Ag@sSiO$_2$@mSiO$_2$-DihBen-Fe^{3+} particles would facilitate the

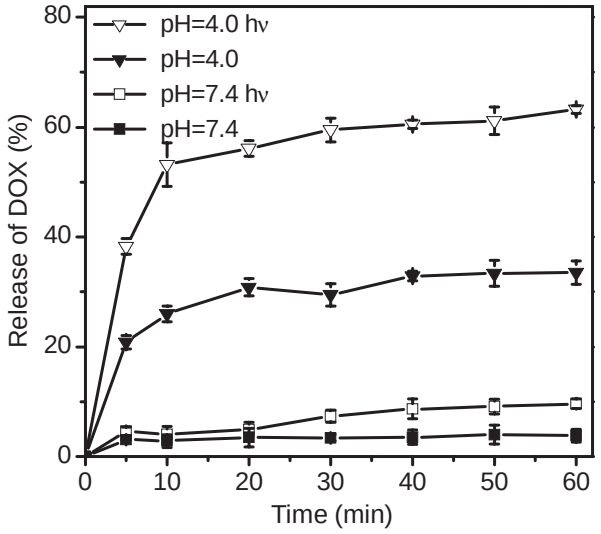

Figure 6. Release kinetics of DOX from Pd@Ag@sSiO$_2$@mSiO$_2$ in PBS buffer at pH values of 7.4 and 4.0 with or without laser irradiation at 808 nm.

cell killing activity of the drug. To confirm such an argument, Hep-G2 cells were incubated with free DOX and DOX-loaded core-shell nanoparticles at different concentrations for 10 h. The MTT assay was then carried out to test cell viabilities. The DOX-loaded core-shell nanoparticles exhibited higher cytotoxicity than free DOX at the same concentrations. While 50 ppm free DOX killed only 36% cells, the same amount of DOX loaded on Pd@Ag@sSiO$_2$@mSiO$_2$-DihBen-Fe^{3+} particles killed 62% cells (Figure 7b, S3). This result can be explained by that DOX-loaded nanoparticles can enter cancer cells more easily than free DOX probably through endocytosis mechanism. Once taken up by living cells, the particles experience a pH drop to ~5.5 or even lower to trigger the release of DOX from the particles.

We have also investigated the feasibility to use NIR laser radiation to enhance the cell-killing efficacy of DOX-loaded Pd@Ag@sSiO$_2$@mSiO$_2$-DihBen-Fe^{3+} particles. In these studies, Hep-G2 cells were first incubated with DOX-loaded nanoparticles for 8 h. After the culture media was replaced by fresh media, the cells were subjected to the NIR irradiation (808 nm, 1 W) for 5 min. After irradiation, the cells were further incubated for 2 h before cell viabilities were determined by MTT. With the NIR irradiation, more cells were killed by DOX-loaded particles at all tested concentrations (Figure 7b and Figure S4 in the Supporting Information). For instance, when exposed to NIR laser, 77% of the cells were killed at the DOX concentration of 20 ppm. In comparison, 46% of the cells were killed in the presence of DOX-loaded particles but the absence of NIR irradiation. In the absence of DOX, Pd@Ag@sSiO$_2$@mSiO$_2$-DihBen-Fe^{3+} under 5-min NIR irradiation killed only 15% of the cells. The cell-killing efficacy by DOX-loaded Pd@Ag@sSiO$_2$@mSiO$_2$-DihBen-Fe^{3+} core–shell particles under NIR irradiation was even higher than the sum of chemotherapy by DOX-loaded Pd@Ag@sSiO$_2$@mSiO$_2$-DihBen-Fe^{3+} particles and photothermal therapy by unloaded Pd@Ag@sSiO$_2$@mSiO$_2$-DihBen-Fe^{3+} particles. This result demonstrates the synergistic effect of combining photothermal therapy and chemotherapy in our core-shell drug delivery system.

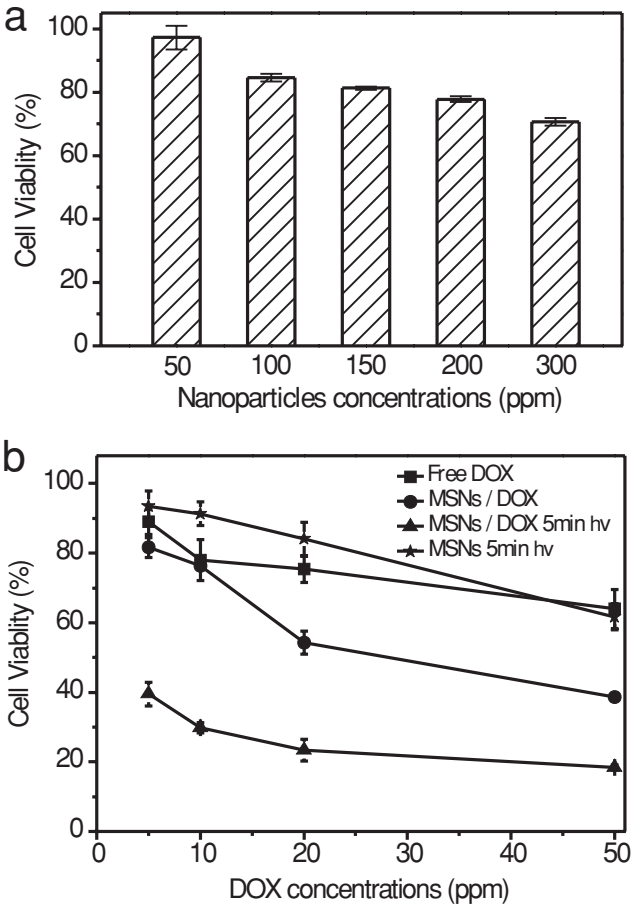

Figure 7. a) Viability of Hep-G2 cells incubated for 24 h with different concentrations of Pd@Ag@sSiO$_2$@mSiO$_2$-DihBen-Fe^{3+} particles. b) Hep-G2 cell viabilities after a 10 h incubation with different concentrations of free DOX, Pd@Ag@sSiO$_2$@mSiO$_2$-DihBen-Fe^{3+} (MSNs) and DOX-loaded Pd@Ag@ sSiO$_2$@mSiO$_2$-DihBen-Fe^{3+} with or without 5-min NIR irradiation (1 W, 808 nm).

3. Conclusions

In summary, a smart anticancer drug delivery system based on Pd@Ag@sSiO$_2$@mSiO$_2$ core–shell particles has been developed. The core–shell architecture allows to integrate the photothermal component (Pd@Ag nanoplates), that can convert NIR light to heat, with the high-surface area component (mesoporous SiO$_2$ shell) for the loading of anticancer drug molecules (DOX). Through coordination bonds that are responsive to pH and heat, the release of DOX from the core–shell particles can be triggered by pH and NIR light, resulting in a synergistic effect for cancer cell killing.

4. Experimental Section

Materials: DOX was purchased from HuaFeng United Technology Co. Ltd. (Beijing, China). Pd(acac)$_2$, tetraethoxysilane (TEOS), 3-aminopropyltrimethoxysilane (APTES) and mesitylene were purchased from Alfa Aesar. 3,4-dihydroxybenzaldehyde, Arg (L-arginine) and CTAC (dodecyltrimethylammonium chloride) were obtained from Sinopharm

Chemical Reagent Co. Ltd. (Shanghai, China). Hep-G2 cells were purchased from cell storeroom of Chinese Academy of Sciences. All reagents were used as received without further purification.

Synthesis of Pd@Ag: Pd and Pd@Ag nanosheets were prepared according to our recently reported method.[16] In brief, the obtained palladium nanosheets (5.79 mg, 4.0 mL solution) were purified by an ethanol-acetone mixture solution, and then dispersed in 45.5 mL of ultrapure water containing 20 mg of $AgNO_3$. After stirred for several minutes, 2.5 mL of formaldehyde solution (40%) was added to the above mixture. The mixture was allowed to react for 8 h at statically to give rise to an ultramarine solution. The resulting solution was stored at 4 °C for future use.

Synthesis of Pd@Ag@sSiO$_2$: 16.0 mL of the above solution containing 6.17 mg of Pd@Ag was mixed with 128 mL of ethanol. 320 µL of TEOS was then added to the mixture, followed by 2.0 mL of methylamine aqueous solution (40%). After reacted for 10 h at room temperature, the product was purified by centrifuging at 14500 rpm for 12 min, washed, and re-dispersed in ethanol.

Synthesis of Pd@Ag@sSiO$_2$@mSiO$_2$: The product was synthesized using a modification of the literature method for the synthesis of mesoporous silica.[17] The above Pd@Ag@$sSiO_2$ nanoparticles were re-dispersed in 120 mL of ultrapure water containing 480 mg of CTAC and 1.2 mL of mesitylene. After ultrasonication for 30 min, 160 µL of TEOS was added, followed by 24.0 mg of Arg (L-arginine) in 1.0 mL of water. The reaction solution was stirred for 24 h at 45 °C before the products were collected by centrifugation, washed with ethanol-water mixed solution and then dispersed in 60 mL of ethanol containing 1.2 g of NH_4NO_3. Finally, the mixture was heated to 45 °C under stirring for 6 h in order to remove surfactant template, the procedures were repeated for three times.

Preparation of Pd@Ag@sSiO$_2$@mSiO$_2$-NH$_2$: 30.0 mg Pd@Ag@$sSiO_2$@$mSiO_2$ nanoparticles, 60.0 mL ethanol, 60.0 µL water and 30.0 µL 3-aminopropyltrimethoxysilane (APTES) were mixed and heated to 45 °C overnight. The product was separated by centrifugation, washed with ethanol and finally re-dispersed in ethanol for subsequent use.

Preparation of Pd@Ag@sSiO$_2$@mSiO$_2$-DihBen-Fe^{3+}: Pd@Ag@$sSiO_2$@$mSiO_2$-NH_2 nanoparticles (4.0 mg) were dispersed in 2.0 mL of ethanol. After that, 0.1 mg of 3, 4-dihydroxybenzaldehyde in ethanol solution was added under stirring. After stirring for 4 h at room temperature, the product was collected by centrifugation and washed with ethanol for one time. The 3,4-dihydroxybenzaldehyde modified Pd@Ag@$sSiO_2$@$mSiO_2$-NH_2 nanoparticles were then re-dispersed in ethanol, followed by adding 120 µL of 0.05 M $Fe(NO_3)_3{\cdot}9H_2O$ ethanol solution. The mixture solution was stirred overnight. Finally, the particles were centrifuged, washed for three times with ethanol and then dispersed in PBS for subsequent use.

DOX Loading and Release Studies: 2.0 mg of Pd@Ag@$sSiO_2$@$mSiO_2$-DihBen-Fe^{3+} nanoparticles were mixed with 1.2 mg of DOX in 1.0 mL of PBS (pH = 7.4), and stirred at room temperature for 36 h. The mixture was centrifuged and washed for three times with PBS (pH = 7.4). To measure the amount of DOX loaded in the core-shell mesoporous nanoparticles, the supernatant solutions containing DOX molecules were measured by the fluorescence spectrum of DOX (ex = 500 nm). The loading capacity of the nanoparticles was determined as the percentage of the weight of DOX related to the weight of Pd@Ag@$sSiO_2$@$mSiO_2$-DihBen-Fe^{3+} nanoparticles. To study the amount of drug releasing from the mesoporous nanoparticles at different pH values, 200 µg of DOX loaded nanoparticles were dispersed in 800 µL of PBS buffer at pH values of 7.4, 6.0, 5.0, 4.0, and shaken at room temperature. The release media solution was collected by centrifugation at a given time for analysis. The amount of DOX molecules in the media solution was then measured by the fluorescence spectrum, and then calculated the releasing percentage of the doxorubicin molecules. To confirm that the drug could controllably release from nanoparticles under laser irradiation at low pH value, 200 µg of DOX loaded nanoparticles were dispersed in 800 µL of PBS buffer at pH values of 7.4 and 4.0 separately, and then illuminated by laser lamp (λ = 808 nm, 1 W). The release media solution was collected at different time for analysis and calculated the released percentage of the doxorubicin molecules. All releasing experiments were repeated three times to obtain the releasing curves. The control experiments were also carried out under the same procedures only without laser irradiation.

Characterization: Transmission electron microscopy (TEM) studies were performed on a TECNAI F-30 high resolution transmission electron microscope operating at 300 kV. Scanning electron microscopy (SEM) images were obtained on Hitachi S4800 scanning electron microscope with a field emission electron gun. Surface area and pore size were determined by Surface Area and Porosity Analyzer (Micromeritics Instrument Corp. ASAP2020).

Cell Culture: Human heatoblastoma cells (Hep-G2) were maintained in Duibecco's modified Eagle's medium (DMEM) supplemented with 10% calf serum, 1% penicillin, 1% streptomycin in 37 °C, 5% CO_2.

Fluorescence Imaging: Hep-G2 cells were seeded in a 24-well plate and cultured for 24 h. The cell medium was removed, and then cells were incubated with 0.5 mL of fresh cell medium containing 20 µg of Pd@Ag@$sSiO_2$@$mSiO_2$-DihBen-Fe^{3+}/DOX nanoparticles for another 4 h. Cell imaging was then carried out after washing cells with PBS.

In Vitro Cytotoxicity Assay: For studying the cytotoxicity of the core-shell mesoporous nanoparticles, Hep-G2 cells were seeded in a 96-well plate at a density 10^4 cells/well for 24 h at 37 °C in 5% CO_2. Then, the cells were treated with free DOX, Pd@Ag@$sSiO_2$@$mSiO_2$–DihBen-Fe^{3+}/DOX or Pd@Ag@$sSiO_2$@$mSiO_2$-DihBen-Fe^{3+} nanoparticles at desired concentration. After incubation for 10 h, cell viabilities were tested by standard MTT (3-(4,5)-dimethylthiahiazo-2-yl)-2,5-diphenyltetrazolium bromide) assay. To confirm that the nanoparticles could efficiently kill cancer cell under laser irradiation, Hep-G2 cells were cultured in 96-well plate for 24 h. After that, the medium was replaced by 200 µL of cell medium with Pd@Ag@$sSiO_2$@$mSiO_2$-DihBen-Fe^{3+}/DOX nanoparticles or free DOX at proper concentration. After maintained for 8 h, the plates were photo-irradiated by a laser lamp (λ = 808 nm, 1 W) for 0 min, 3 min, 5 min. Cell viabilities were also tested by standard MTT assay. To identify the cell viability, the dead cells were stained with Trypan Blue.

Supporting Information

Supporting Information is available from the Wiley Online Library or from the author.

Acknowledgements

We thank the NSFC (21131005, 21021061, 20925103), the Fok Ying Tung Education Foundation (121011), the MOST of China (2011CB932403, 2009CB930703), NFFTBS (J1030415), and the NSF of Fujian Province (Distinguished Young Investigator Grant 2009J06005) for the financial support.

Received: August 20, 2011
Revised: November 3, 2011
Published online: December 13, 2011

[1] a) E. A. Rozhkova, *Adv. Mater.* **2011**, *23*, H136–H150; b) C. Minelli, S. B. Lowe, M. M. Stevens, *Small* **2010**, *6*, 2336–2357.
[2] a) R. Duncan, *Nat. Rev. Cancer* **2006**, *6*, 688–701; b) C. Li, S. Wallace, *Adv. Drug. Delivery Rev.* **2008**, *60*, 886–898; c) N. Nishiyama, K. Kataoka, *Pharmacol. Ther.* **2006**, *112*, 630–648.
[3] a) C. Sahlgren, J. M. Rosenholm, M. Linden, *Nanoscale* **2010**, *2*, 1870–1883; b) I. I. Slowing, Y. N. Zhao, J. L. Vivero-Escoto, B. C. Trewyn, V. S. Y. Lin, *Expert Opin. Drug Delivery* **2010**, *7*, 1013–1029.
[4] J. F. Stoddart, K. C. F. Leung, T. D. Nguyen, J. I. Zink, *Chem. Mater.* **2006**, *18*, 5919–5928.

[5] a) L. Du, S. Liao, H. A. Khatib, J. F. Stoddart, J. I. Zink, *J. Am. Chem. Soc.* **2009**, *131*, 15136–15142; b) Q. Gao, Y. Xu, D. Wu, W. Shen, F. Deng, *Langmuir* **2010**, *26*, 17133–17138; c) R. Liu, Y. Zhang, X. Zhao, A. Agarwal, L. J. Mueller, P. Feng, *J. Am. Chem. Soc.* **2010**, *132*, 1500–1501; d) H. Meng, M. Xue, T. Xia, Y. L. Zhao, F. Tamanoi, J. F. Stoddart, J. I. Zink, A. E. Nel, *J. Am. Chem. Soc.* **2010**, *132*, 12690–12697; e) Y. L. Zhao, Z. Li, S. Kabehie, Y. Y. Botros, J. F. Stoddart, J. I. Zink, *J. Am. Chem. Soc.* **2010**, *132*, 13016–13025.
[6] S. L. Brock, Y. Z. You, K. K. Kalebaila, D. Oupicky, *Chem. Mater.* **2008**, *20*, 3354–3359.
[7] a) C. Park, H. Kim, S. Kim, C. Kim, *J. Am. Chem. Soc.* **2009**, *131*, 16614–16615; b) J. S. Ren, C. E. Chen, J. Geng, F. Pu, X. J. Yang, X. G. Qu, *Angew. Chem. Int. Ed.* **2011**, *50*, 882–886.
[8] a) C. Y. Lai, B. G. Trewyn, D. M. Jeftinija, K. Jeftinija, S. Xu, S. Jeftinija, V. S. Lin, *J. Am. Chem. Soc.* **2003**, *125*, 4451–4459; b) T. D. Nguyen, Y. Liu, S. Saha, K. C. Leung, J. F. Stoddart, J. I. Zink, *J. Am. Chem. Soc.* **2007**, *129*, 626–634.
[9] a) P. Y. Feng, R. Liu, Y. Zhang, *J. Am. Chem. Soc.* **2009**, *131*, 15128–15129; b) Q. Lin, Q. Huang, C. Li, C. Bao, Z. Liu, F. Li, L. Zhu, *J. Am. Chem. Soc.* **2010**, *132*, 10645–10647.
[10] a) N. K. Mal, M. Fujiwara, Y. Tanaka, *Nature* **2003**, *421*, 350–353; b) N. K. Mal, M. Fujiwara, Y. Tanaka, T. Taguchi, M. Matsukata, *Chem. Mater.* **2003**, *15*, 3385–3394.
[11] F. Tamanoi, J. Lu, E. Choi, J. I. Zink, *Small* **2008**, *4*, 421–426.
[12] a) V. S. Y. Lin, J. L. Vivero-Escoto, I. I. Slowing, C. W. Wu, *J. Am. Chem. Soc.* **2009**, *131*, 3462–2463; b) J. Lai, X. Mu, Y. Xu, X. Wu, C. Wu, C. Li, J. Chen, Y. Zhao, *Chem. Commun.* **2010**, *46*, 7370–7372.
[13] a) D. J. Hawrysz, E. M. Sevick-Muraca, *Neoplasia* **2000**, *2*, 388–417; b) R. Weissleder, *Nat. Biotechnol.* **2001**, *19*, 316–317.
[14] a) C. Y. Bao, Q. N. Lin, Q. Huang, C. Y. Li, Z. Z. Liu, F. Y. Li, L. Y. Zhu, *J. Am. Chem. Soc.* **2010**, *132*, 10645–10647; b) M. D. Marcos, E. Aznar, R. Martinez-Manez, F. Sancenon, J. Soto, P. Amoros, C. Guillem, *J. Am. Chem. Soc.* **2009**, *131*, 6833–6843.
[15] X. Huang, S. Tang, X. Mu, Y. Dai, G. Chen, Z. Zhou, F. Ruan, Z. Yang, N. Zheng, *Nat. Nanotech.* **2011**, *6*, 28–32.
[16] X. Huang, S. Tang, B. Liu, B. Ren, N. Zheng, *Adv. Mater.* **2011**, *23*, 3420–3425.
[17] T. Tatsumi, T. Yokoi, T. Karouji, S. Ohta, J. N. Kondo, *Chem. Mater.* **2010**, *22*, 3900–3908.
[18] a) J. Liu, S. Z. Qiao, S. Budi Hartono, G. Q. Lu, *Angew. Chem. Int. Ed.* **2010**, *49*, 4981–4985; b) X. Fang, C. Chen, Z. Liu, P. Liu, N. Zheng, *Nanoscale* **2011**, *3*, 1632–1639.
[19] S. N. Che, C. B. Gao, H. Q. Zheng, L. Xing, M. H. Shu, *Chem. Mater.* **2010**, *22*, 5437–5444.
[20] a) Z. Liu, J. T. Robinson, X. Sun, H. Dai, *J. Am. Chem. Soc.* **2008**, *130*, 10876–10877; b) S. H. Tang, X. Q. Huang, X. L. Chen, N. F. Zheng, *Adv. Funct. Mater.* **2010**, *20*, 2442–2447.